Theoretical prediction of noble-gas compounds: Ng–Pd–Ng and Ng–Pt–Ng

Yuriko Taketsugu, Tetsuya Taketsugu,[a] and Takeshi Noro
Division of Chemistry, Graduate School of Science, Hokkaido University, Sapporo 060-0810, Japan

(Received 5 July 2006; accepted 5 September 2006; published online 18 October 2006)

Following our recent study on Ng–Pt–Ng (Ng=Ar,Kr,Xe) [J. Chem. Phys. **123**, 204321 (2005)], the binding of noble-gas atoms with Pd atom has been investigated by the *ab initio* coupled cluster CCSD(T) method with counterpoise corrections, including relativistic effects. It is shown that two Ng atoms bind with Pd atom in linear geometry due to the s-d_σ hybridization in Pd where the second Ng atom attaches with much larger binding energy than the first. The binding energies are evaluated as 4.0, 10.2, and 21.5 kcal/mol for Ar–Pd–Ar, Kr–Pd–Kr, and Xe–Pd–Xe, respectively, relative to the dissociation limit, Pd $(^1S)+2$Ng. In the hybrid Ng complexes, the binding energies for XePd and Ng (=Ar,Kr) are evaluated as 4.0 and 6.9 kcal/mol for XePd–Ar and XePd–Kr, respectively. The fundamental frequencies and low-lying vibrational-rotational energy levels are determined for each compound by the variational method, based on the three-dimensional near-equilibrium potential energy surface. Results of vibrational-rotational analyses for Ng–Pt–Ng (Ng=Ar,Kr,Xe) and Xe–Pt–Ng (Ng=He,Ne,Ar,Kr) compounds are also given. © *2006 American Institute of Physics*. [DOI: 10.1063/1.2358356]

I. INTRODUCTION

Chemical compounds containing noble-gas atoms have attracted much attention since the synthesis of the first Ng compound, $XePtF_6$.[1] In the field of noble-gas chemistry, there has been a lot of interplay between the experiments and theoretical calculations. Frenking and co-workers[2–4] first predicted the existence of neutral species containing a light noble-gas atom, Ng–BeO (Ng=He,Ne,Ar), by *ab initio* calculations. Later, the compounds, Ng–BeO (Ng=Ar,Kr,Xe), have been detected experimentally by Thompson and Andrews through pulsed-laser-ablation matrix-isolation spectroscopy,[5] and then Veldkamp and Frenking[6] reported the calculated structures and bond energies for those detected compounds. Very recently, we reported theoretical calculations that an argon atom possibly combines with NiCO, NiN_2, and CoCO, with a larger binding energy than expected (7–9 kcal/mol).[7–10] It was shown that the bending frequency in these compounds increases by 40–50 cm^{-1} (~10%) due to binding with an argon atom, resulting in quite good agreements with the corresponding experimental frequencies recorded for each compound in solid argon.

Pyykkö predicted the existence of gold-xenon cationic species, $AuXe^+$ and $XeAuXe^+$, by theoretical calculations,[11] which have been detected later by mass sepectroscopy.[12] The binding strength in a noble-gas–noble-metal bond, Au–Xe, has been related to the strong relativistic effects in heavy elements.[13,14] In 2000, Seidel and Seppelt[15] reported the existence of bulk compound, $AuXe_4^{2+}[Sb_2F_{11}^-]_2$. Hu and Huang[16] studied the intrinsic stability of the noble-gas-coordinated transition metal complex ions, $[AuNg_4]^{2+}$ (Ng=Ar,Kr,Xe), and some other hypothetical ions by density functional theory (DFT) and *ab initio* calculations. Gerry and co-workers have found that Ng atom makes a stable compound with a coinage metal monohalide, Ng–MX (Ng=Ar,Kr,Xe; M=Cu,Ag,Au; and X=F,Cl,Br) and determined their geometrical structures by the microwave spectra.[17–23] An *ab initio* study on these compounds showed a qualitative agreement in bond lengths between theory and experiment.[24] Ghanty proposed a new class of Ng compounds containing noble-gas–noble-metal bond where Ng atom is inserted into a noble-metal molecule (Au–X) resulting in the formation of Au–Ng–X species and investigated the stability of Au–Ng–X (Ng=Kr,Xe; X=F,OH)[25] and M–Ng–F (M=Ag,Cu; Ng=Ar,Kr,Xe)[26] by DFT and *ab initio* calculations.

Burda *et al.*[27] investigated a binding strength for the neutral species, M–Xe (M=Ni,Pd,Pt), by applying *ab initio* methods with quasirelativistic pseudopotentials. They found that Pd–Xe and Pt–Xe were bound by 9.9 and 16.2 kcal/mol, respectively, while Ni–Xe has no bound states. Very recently we also examined the binding of Pt atom with noble-gas atoms, Ar, Kr, and Xe, by *ab initio* coupled cluster method with the larger all-electron basis sets and found that two Ng atoms can bind with Pt atom strongly in linear geometry in the singlet lowest state where the second Ng atom attaches to Pt atom with a larger binding energy than the first Ng atom.[28] The binding energies were evaluated as 8.2, 17.9, and 33.4 kcal/mol for Ar–Pt–Ar, Kr–Pt–Kr, and Xe–Pt–Xe, respectively, relative to the triplet ground state of the dissociation limit, Pt $(^3D)+2$Ng.

In the present study, we investigate geometrical structures and binding energies of new noble-gas-containing species, Pd–Ng, Pd–Ng_2, and Pd–Ng_3 (Ng=Ar,Kr,Xe), by applying *ab initio* coupled cluster calculations with the large basis sets, including relativistic effects. The possibility of existence of the hybrid Ng compounds, Xe–Pd–Ng (Ng=He,Ne,Ar,Kr), is also examined. To help the spectro-

[a]Author to whom correspondence should be addressed. Fax: +81 11 706 3535. Electronic mail: take@sci.hokudai.ac.jp.

scopic search of these new species, fundamental frequencies, overtones, and combination bands are evaluated for triatomic compounds by the variational method using the RVIB3 program developed by Carter and Handy.[29,30] Similar vibrational-rotational analysis is also performed for platinum–noble-gas triatomic molecules.

II. COMPUTATIONAL DETAILS

Ab initio calculations were carried out for the singlet ground state of Pd–Ng (in $C_{\infty v}$), Pd–Ng_2 (in $D_{\infty h}$), and Pd–Ng_3 (in D_{3h}) (Ng=Ar,Kr,Xe), as well as the hybrid complex, Xe–Pd–Ng (Ng=He,Ne,Ar,Kr), at the coupled cluster singles and doubles including a perturbational estimate of triple excitations [CCSD(T)] level using the MOLPRO program package.[31] In the CCSD calculations, inner-shell orbitals were frozen for noble-gas atoms, while the excitations from 4*s*, 4*p*, and 4*d* orbitals were taken into account explicitly for Pd atom. The relativistic effects were included by using the Douglas-Kroll relativistic one-electron integrals.[32,33] We also calculated the energy level of Pd (^3D) by the spin-restricted CCSD(T) [RCCSD(T)] method to check the accuracy of the present computational methods.

We have used the relativistic basis sets developed by Tsuchiya *et al.*[34] for the inner and valence shells, which are augmented by the correlated sets of basis functions developed by Sekiya and co-workers.[35–39] The original basis set of Tsuchiya *et al.* for Pd atom is a minimal one which is written as $(23s19p12d)/[4s3p2d]$. This set has been split and the correlated sets[35] have been added so as to represent the effect of electron correlation due to 4*s*, 4*p*, and 4*d* orbitals of Pd atom, i.e., $(23,23,23,23)+(3,1,2)\rightarrow(20,20,20,20,1,1,1,3,1,2)$ for *s* function, $(19,19,19)\rightarrow(15,15,15,1,1,1,1)$ for *p* function, and $(12,12)+(6,2,2,1)\rightarrow(8,6,1,1,1,1,1)$ for *d* function [(12,12) sets of Tsuchiya *et al.* have been reduced to (8) to represent 3*d* orbitals, and (6,2,2,1) sets of Sekiya and co-workers for 4*d* orbitals and correlated sets have been added and split]. The correlated sets of (2,1) *f* and (2) *g* functions have also been added.[32] As to the basis sets for Ng atoms, the original basis sets of Tsuchiya *et al.* are split in valence parts of *s* and *p* functions as $(6)\rightarrow(3,1,1,1)$ for He, $(12,12/8)\rightarrow(9,9,1,1,1/5,1,1,1)$ for Ne, $(16,16,16/11,11)\rightarrow(13,13,13,1,1,1/8,8,1,1,1)$ for Ar, $(20,20,20,20/15,15,15/9)\rightarrow(17,17,17,17,1,1,1/12,12,12,1,1,1/9)$ for Kr, and $(23,23,23,23,23/19,19,19,19/12,12)\rightarrow(21,21,21,21,21,1,1/16,16,16,16,1,1,1/12,12)$ for Xe, and the correlated sets, $(p/d/f)=(2,1,1/2,1/2)$ for He,[36] $(d/f/g)=(2,1,1/2,1/2)$ for Ne,[36] $(d/f/g)=(3,1,1/1,1/2)$ for Ar,[37] $(1,1,1/1,1/2)$ for Kr,[38] and $(1,1/1,1/2)$ for Xe,[38] are added.

In the estimation of the interaction energy between Pd and Ng atoms, the basis set superposition error (BSSE) was corrected by the standard counterpoise correction method.[40] The interaction energy (V_{int}) for Pd–Ng, Pd–Ng_2, and Pd–Ng_3 can be expressed respectively as

$$V_{\mathrm{int,Pd-Ng}}(r)=V_{\mathrm{Pd-Ng}}(r)-V_{\mathrm{Pd}}(r)-V_{\mathrm{Ng}}(r), \tag{1}$$

$$V_{\mathrm{int,Pd-Ng_2}}(r)=V_{\mathrm{Pd-Ng_2}}(r)-V_{\mathrm{Pd}}(r)-V_{\mathrm{Ng}}(r)\times 2, \tag{2}$$

$$V_{\mathrm{int,Pd-Ng_3}}(r)=V_{\mathrm{Pd-Ng_3}}(r)-V_{\mathrm{Pd}}(r)-V_{\mathrm{Ng}}(r)\times 3, \tag{3}$$

where $V_x(r)$ denotes the CCSD(T) energy for *X* system or fragment with the Pd–Ng distance *r* calculated with the basis sets for the entire system. Geometry optimizations are carried out within the respective point groups by minimizing the above interaction energies in Eqs. (1)–(3). The binding energy is evaluated as the interaction energy $V_{\mathrm{int},X}(r_{\mathrm{eq}})$ at the optimized structures. Normal mode analyses are performed for Pd–Ng and Pd–Ng_2 by numerical differentiations of the counterpoise-corrected interaction energy $V_{\mathrm{int},X}$ for the most probable isotopic species (^{106}Pd, ^{40}Ar, ^{84}Kr, and ^{132}Xe).

For triatomic compounds, Pd–Ng_2 (Ng=Ar,Kr,Xe) and Xe–Pd–Ng (Ng=He,Ne,Ar,Kr), we also carried out variational calculations to determine fundamental frequencies and low-lying vibrational energy levels using the RVIB3 code[29,30] in terms of three-dimensional interaction potential energy surfaces. To determine the potential energy surface, we calculated CCSD(T) counterpoise-corrected energies at 196 points around the equilibrium structure and then fitted those energies to the fourth-order polynomials as

$$V(q_1,q_2,q_3)=\sum_{i,j,k} C_{ijk}q_1^i q_2^j q_3^k \quad (i,j,k=0-4), \tag{4}$$

where q_1 and q_2 denote the dimensionless Simons-Parr-Finlan coordinate for each Pd–Ng bond length (r_1 and r_2) defined as[41]

$$q_i=\frac{r_i-r_{\mathrm{eq}}}{r_i}, \tag{5}$$

and q_3 denotes the supplement of the valence angle in radian. For Pd–Ng_2 species in $D_{\infty h}$ point group, the symmetry-adapted stretching coordinates were used in RVIB3 calculations. The basis functions for the stretching part have been built by contracting 25 one-dimensional harmonic oscillator functions for each stretching coordinate to 16 functions in terms of 46 Gauss-Hermite quadrature points and combining these optimized functions in a series of two-dimensional contraction schemes; the size of the Hamiltonian matrix is $16\times 16=256$ which is split to sub-blocks of totally symmetric and antisymmetric parts in the case of $D_{\infty h}$ species, and 16 two-dimensional functions were collected in the respective symmetry representations. As to the bending part, 71 associated Legendre functions have been employed as the primitive basis functions, which were then contracted to 35 basis functions; the optimized bending functions were stored at 82 quadrature points. For each value of the rotational quantum number, the secular matrix was constructed using the vibrational expansion functions and the rotational symmetric-top functions and was diagonalized to obtain the vibrational-rotational energy levels.

We also carried out additional calculations for the platinum–noble gas compounds, Pt–Ng_2 (Ng=Ar,Kr,Xe) and Xe–Pt–Ng (Ng=He,Ne,Ar,Kr), at the same computational levels. The basis sets for Pt have been made from the

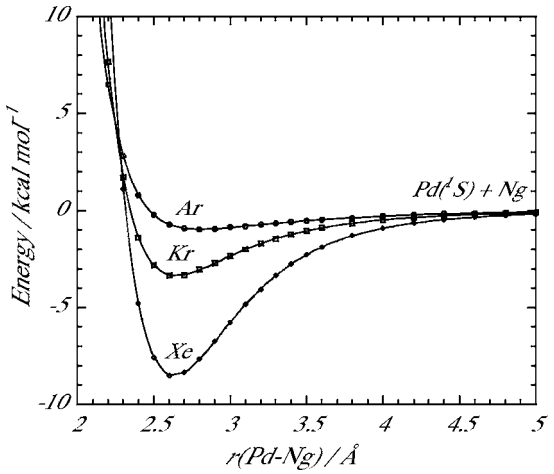

FIG. 1. Potential energy curves for the singlet ground state ($^1\Sigma^+$) of Pd–Ng (Ng=Ar,Kr,Xe).

relativistic basis sets[34] and the correlated sets,[39] the details of which are described in the previous paper.[28] The calculations include geometry optimization and vibrational-rotational calculations using the RVIB3 code for the respective compounds.

III. RESULTS AND DISCUSSION

The electronic ground state of Pd atom is ^1S, with the valence electronic configuration $(4d)^{10}$ while the first excited state is ^3D with $(4d)^9(5s)^1$. By CCSD(T) and RCCSD(T) calculations, the energy difference between ^1S and ^3D states of Pd atom is evaluated as 19.2 kcal/mol, which is smaller by about 1 kcal/mol than the experimental (*J*-averaged) value from the NIST tables, 20.3 kcal/mol.[42] Raab and Roos reported the closer value, 19.8 kcal/mol, for the corresponding excitation energy calculated by the CCSD(T) method with different basis sets.[43] In the case of Pt atom the electronic ground state is ^3D $[(5d)^9(6s)^1]$, while the first excited state is ^1S $[(5d)^{10}]$. Their energy difference was evaluated as 11.5 kcal/mol at the same computational level.[28] By the binding with Ng atoms, the triplet potential energy curves for Pt–Ng show a repulsive feature, while the singlet state is stabilized, resulting in the bound $^1\Sigma^+$ ground state of Pt–Ng. Then, the triplet and singlet potential energy curves cross with each other at some interatomic distance in Pt–Ng, while such curve crossings do not occur in Pd–Ng. In Pd–Ng system, the spin-orbit coupling effects from the triplet excited state on the singlet ground-state potential energy curve may be very small because of a sufficiently large energy difference. Therefore we focus on the singlet ground state of palladium–noble-gas compounds in the following.

Figure 1 shows potential energy curves, $V_{\text{int,Pd–Ng}}$, for the ground $^1\Sigma^+$ state of Pd–Ng (Ng=Ar,Kr,Xe). In these potential energy curves, the BSSE was already corrected by the counterpoise method. As shown in Fig. 1, the respective compounds have bound states. The binding energies are evaluated as 0.94 kcal/mol for PdAr, 3.35 kcal/mol for PdKr, and 8.52 kcal/mol for PdXe, while the equilibrium bond distances are 2.797, 2.643, and 2.629 Å for PdAr, PdKr, and PdXe, respectively. Without the counterpoise corrections, the corresponding equilibrium bond lengths are calculated as 2.685, 2.596, and 2.603 Å, and the binding energies are calculated as 1.60, 4.40, and 10.05 kcal/mol for PdAr, PdKr, and PdXe, respectively. The BSSE makes the binding energy larger by 0.6–1.5 kcal/mol, and thus, it is important to correct the BSSE in these systems. In previous CCSD(T) calculations with pseudopotentials for PdXe,[27] the binding energy was evaluated as 9.9 kcal/mol, and the equilibrium bond length was calculated as 2.52 Å, indicating a slightly stronger binding between Pd and Ng atoms than our results. Table I summarizes the equilibrium bond lengths, binding energies, rotational constants, and harmonic frequencies for Pd–Ng derived from CCSD(T) counterpoise-corrected potential energy curves, as well as Mulliken atomic-orbital populations and dipole moments at the CCSD level. The harmonic frequencies are calculated as 53.9 cm^{-1} (PdAr), 96.0 cm^{-1} (PdKr), and 132.1 cm^{-1} (PdXe), and the binding energies including zero-point vibrational energy are evaluated as 0.86 kcal/mol (PdAr), 3.21 kcal/mol (PdKr), and 8.34 kcal/mol (PdXe). For comparison, the corresponding values for Pt–Ng reported previously[28] are also given in Table I where the binding energy is given relative to $Pt(^1S)+Ng(^1S)$. It is evident that Pt–Ng binding is stronger than the corresponding Pd–Ng bonding both in terms of bond length and binding energy. It is interesting to note that the Pt–Ng bond lengths are smaller than the corresponding Pd–Ng bond lengths, although Pt and Pd belong to the same group of the

TABLE I. Equilibrium bond lengths (r_e), binding energies (BE_e and BE_0), rotational constants (B_e), harmonic frequencies (ω), and Mulliken atomic-orbital populations for Pd–5*s* and Pd–4*d* (*n*), and dipole moment (μ) calculated for the singlet ground state of Pd–Ng. For comparison, the corresponding values for Pt–Ng reported recently are also shown where Mulliken atomic-orbital populations for Pt–6*s* and Pt–5*d* at the CCSD level are given.

Parameter	Pd–Ar	Pd–Kr	Pd–Xe	Pt–Ar[a]	Pt–Kr[a]	Pt–Xe[a]
r_e (Å)	2.797	2.643	2.629	2.383	2.430	2.500
BE_e (kcal/mol)	0.94	3.35	8.52	7.25	12.77	22.10
BE_0 (kcal/mol)	0.86	3.21	8.34	6.99	12.53	21.85
B_e (GHz)	2.398	1.596	1.271	2.685	1.459	1.028
ω (cm^{-1})	53.9	96.0	132.1	184.7	168.8	172.6
n(Pd–5*s*), n(Pt–6*s*)	0.034	0.082	0.142	0.396	0.434	0.481
n(Pd–4*d*), n(Pt–5*d*)	9.863	9.804	9.727	9.505	9.478	9.445
μ (D)	0.28	0.32	0.26	0.65	0.84	0.97

[a]Reference 28.

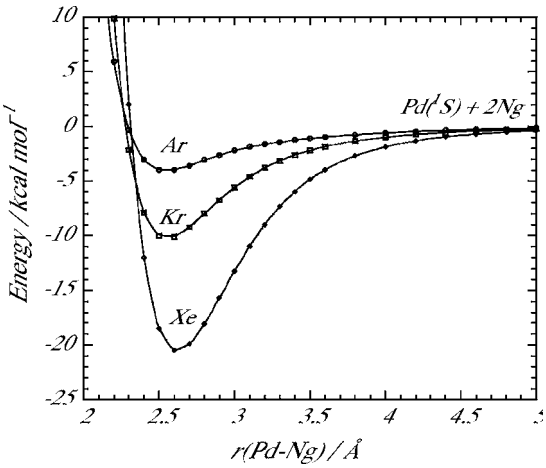

FIG. 2. Potential energy curves for the singlet ground state ($^1\Sigma_g^+$) of $Pd-Ng_2$ (Ng=Ar,Kr,Xe) in $D_{\infty h}$ point group as a function of Pd–Ng distance r(PdNg).

Periodic Table and Pt is just below Pd. Certainly this is linked with the stronger relativistic effect in Pt and is a consequence of relativistic bond length contraction as discussed by Pyykkö and Desclaux[13] and Pyykkö.[14]

Here we discuss the binding mechanism of Pd and Ng atoms. As shown in Table I, Pd-5s population slightly increases ($0 \rightarrow 0.142$) while Pd-4d population slightly decreases ($10 \rightarrow 9.727$) in Pd–Ng (numbers in parentheses correspond to populations for Pd–Xe). This means that, by the binding with Ng atom, the s-d_σ hybridization is invoked in Pd atom due to the mixing of $(4d)^{10}$ and $(4d)^9(5s)^1$ electronic configurations. The s-d_σ hybridization moves Pd-d_σ electrons out into regions perpendicular to the Pd–Ng axis, which leads to an electron-nuclear attraction between a partially unshielded Pd core and the electrons on Ng atom. This may be the origin of the binding strength between Pd and Ng atoms. The same mechanism was previously proposed for understanding the metal-ligand binding mechanism in Pd-H_2O and in Pd-NH_3 by Blomberg and co-workers.[44,45]

For $Pd-Ng_2$ systems, the counterpoise corrections have been applied to evaluate the binding energy relative to the dissociation limit of Pd+Ng+Ng in the same way as calculations for Pd–Ng. Figure 2 shows counterpoise-corrected potential energy curves, $V_{\mathrm{int,Pd-Ng_2}}$, for the lowest singlet ($^1\Sigma^+$) state of $Pd-Ng_2$ (Ng=Ar,Kr,Xe) in $D_{\infty h}$ configuration as a function of Pd–Ng distance. As shown in the potential energy curves, these compounds have a large binding energy, i.e., 4.01, 10.17, and 21.49 kcal/mol for $Pd-Ar_2$, $Pd-Kr_2$, and $Pd-Xe_2$, respectively. The binding energies for Pd–Ng are evaluated as 0.94 kcal/mol (Pd–Ar), 3.35 kcal/mol (Pd–Kr), and 8.52 kcal/mol (Pd–Xe) as shown in Table I, and thus, the additional binding energy for the second Ng atom is much larger than that for the first Ng atom in all cases: 3.07 kcal/mol ($PdAr_2$), 6.82 kcal/mol ($PdKr_2$), and 12.97 kcal/mol ($PdXe_2$). Table II summarizes the equilibrium bond length, binding energies [without and with zero-point vibrational energy (ZPE) correction], and rotational constants (equilibrium one and effective one for ZPE level) for ($PdNg_2$), as well as Mulliken atomic-orbital populations for Pd-5s and Pd-4d at the CCSD level. The corresponding data for Pt-Ng_2 are also given where the binding energy is given relative to $Pt(^1S)+2Ng(^1S)$. The equilibrium bond lengths are calculated as 2.544, 2.554, and 2.619 Å for $Pd-Ar_2$, $Pd-Kr_2$, and $Pd-Xe_2$, respectively, and so the order in bond lengths is reverse between Pd–Ng and $Pd-Ng_2$. The changes in Pd–Ng bond lengths indicate that the binding between Ng and Pd becomes much stronger especially for $Pd-Ar_2$ and $Pd-Kr_2$ than the corresponding Pd–Ng diatomic molecules. The corresponding Pt–Ng bond lengths are 2.352, 2.435, and 2.546 Å for $Pt-Ar_2$, $Pt-Kr_2$, and $Pt-Xe_2$, respectively. The shorter bond lengths in $Pt-Ng_2$ indicate the larger contributions of relativistic effects in $Pt-Ng_2$ than in $Pd-Ng_2$, as is the case for Pd–Ng and Pt–Ng molecules.

In order to get insight into the higher bond strength of the second Pd–Ng bond in $Pd-Ng_2$, we calculated the potential energy curve for XePd–Xe′ as a function of Pd–Xe′ interatomic distance r, where XePd bond length is fixed to the equilibrium bond length in $PdXe_2$. In this calculation, the counterpoise-corrected interaction energy was evaluated as

$$V_{\mathrm{int,Xe-Pd-Xe'}}(r) = V_{\mathrm{Xe-Pd-Xe'}}(r) - V_{\mathrm{Pd}}(r) - V_{\mathrm{Xe}}(r) - V_{\mathrm{Xe'}}(r). \quad (6)$$

Figure 3 shows the calculated potential energy curves for $XePd-Xe' \rightarrow XePd+Xe'$ and $PdXe \rightarrow Pd+Xe$. Dashed lines denote the energy levels of Pd+2Xe, XePd+Xe, and XePdXe. The potential energy curve for $XePd-Xe' \rightarrow XePd+Xe'$ shows a minimum at the $D_{\infty h}$ equilibrium bond length, indicating that the $D_{\infty h}$ equilibrium structure of $Pd-Xe_2$ cor-

TABLE II. The equilibrium bond length, binding energies, rotational constants, and Mulliken atomic-orbital populations for Pd–5s and Pd–4d for $Pd-Ng_2$. For comparison, the corresponding values for $Pt-Ng_2$ reported recently are also shown where Mulliken atomic-orbital populations for Pt–6s and Pt–5d at the CCSD level are given.

Parameter	$Pd-Ar_2$	$Pd-Kr_2$	$Pd-Xe_2$	$Pt-Ar_2$[a]	$Pt-Kr_2$[a]	$Pt-Xe_2$[a]
r_e (Å)	2.544	2.554	2.619	2.352	2.435	2.546
BE_e (kcal/mol)	4.01	10.17	21.49	19.65	29.43	44.92
BE_0 (kcal/mol)	3.56	9.70	21.00	18.76	28.74	44.31
B_e (GHz)	0.9770	0.4617	0.2793	1.1392	0.5060	0.2954
B_0 (GHz)	0.9612	0.4588	0.2785	1.1324	0.5044	0.2949
n(Pd–5s), n(Pt–6s)	0.196	0.260	0.328	0.676	0.710	0.75
n(Pd–4d), n(Pt–5d)	9.688	9.617	9.539	9.267	9.265	9.20

[a]Reference 28.

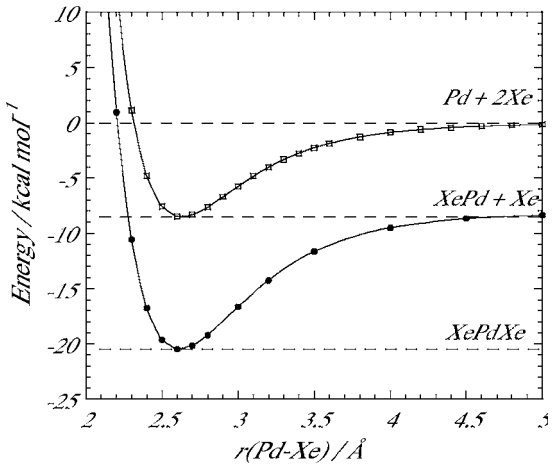

FIG. 3. Potential energy curves for XePd−Xe→XePd+Xe and PdXe →Pd+Xe as a function of Pd–Xe distance r(PdXe). Dashed lines denote the energy levels of Pd+2Xe, XePd+Xe, and XePdXe.

responds to a global minimum. As is clearly shown in these potential energy curves, the second Xe atom attaches to XePd with a larger binding energy than the first Xe atom.

Why does the second Ng atom bind stronger than the first one? This can also be explained by the s-d_σ hybridization in Pd atom. As described for the Pd–Ng diatomic molecules, the s-d_σ hybridization reduces the charge density along the molecular axis, and thus electron repulsions between Pd and Ng atoms are reduced. In Ng–Pd–Ng, both Ng atoms benefit from reduced repulsion, while they can share the energetic cost of hybridization. This is the reason why the second Ng atom attaches to Pd–Ng from the other side in the linear configuration more strongly than the first Ng atom. The similar interpretation was applied previously to explain the tendency in the binding energies of $Cu^+-(H_2O)_n$ and $Cu^+-(NH_3)_n$.[46,47] According to the atomic-orbital populations of Pd−5s and Pd−4d in Tables I and II, the s-d_σ hybridization is invoked much stronger in Pd−Ng_2 than in Pd–Ng.

For Pd−Ng_2, the harmonic frequencies were also calculated by numerical differentiations of CCSD(T) counterpoise-corrected energies. All the frequencies are given in real number, indicating that Pd−Ng_2 takes a $D_{\infty h}$ linear geometry as the equilibrium structure. The ZPEs were evaluated from variational RVIB3 calculations as 158.7, 166.2, and 170.9 cm^{-1} for Pd−Ar_2, Pd−Kr_2, and Pd−Xe_2, respectively, and then, the binding energy BE_0 was calculated as 3.56, 9.70, and 21.00 kcal/mol, respectively. The comparison of B_e and B_0 rotational constants indicates that the anharmonic effect seems not so strong in Pd−Kr_2 and Pd−Xe_2 compared to that in Pd−Ar_2. Table III gives the expansion coefficients for the potential energy surfaces defined in Eq. (4), determined for $M-Ng_2$(M=Pd,Pt;Ng =Ar,Kr,Xe). In this table, only symmetrically unique coefficients are given (due to $D_{\infty h}$ point group, $C_{020}=C_{200}$, $C_{120}=C_{210}$, and so on). The second-order terms, C_{200} and C_{002}, correspond to the harmonic force constants of M−Ng bond (in Simons-Parr-Finlan coordinate) and Ng−M−Ng valence angle. The comparison of C_{200} indicates that the relative ratio in the strength of Pd–Ng bond is almost 1 (Ar):2 (Kr):3 (Xe), while C_{002} coefficients show relatively close value in three compounds.

TABLE III. Expansion coefficients for potential energy surfaces of Pd−Ng_2 and Pt−Ng_2.

				Pd−Ar_2			
C_{200}	0.194 407	C_{110}	−0.078 961	C_{002}	0.007 742	C_{300}	−0.763 204
C_{210}	−0.071 865	C_{102}	−0.033 643	C_{400}	1.037 370	C_{310}	0.327 223
C_{220}	−0.005 677	C_{202}	0.028 158	C_{112}	0.151 308	C_{004}	−0.001 989
				Pd−Kr_2			
C_{200}	0.358 097	C_{110}	−0.041 161	C_{002}	0.010 780	C_{300}	−1.223 458
C_{210}	−0.175 580	C_{102}	−0.039 966	C_{400}	1.264 763	C_{310}	0.312 456
C_{220}	0.058 079	C_{202}	0.014 216	C_{112}	0.163 238	C_{004}	−0.002 518
				Pd−Xe_2			
C_{200}	0.552 781	C_{110}	0.096 090	C_{002}	0.012 197	C_{300}	−1.771 558
C_{210}	−0.401 047	C_{102}	−0.038 052	C_{400}	1.623 847	C_{310}	0.073 091
C_{220}	0.678 666	C_{202}	−0.005 235	C_{112}	0.138 648	C_{004}	−0.002 190
				Pt−Ar_2			
C_{200}	0.567 741	C_{110}	0.027 104	C_{002}	0.033 163	C_{300}	−1.732 442
C_{210}	−0.425 301	C_{102}	−0.087 268	C_{400}	1.295 132	C_{310}	0.494 255
C_{220}	1.050 936	C_{202}	−0.028 275	C_{112}	0.333 208	C_{004}	−0.008 484
				Pt−Kr_2			
C_{200}	0.734 199	C_{110}	0.108 766	C_{002}	0.032 262	C_{300}	−2.143 897
C_{210}	−0.413 984	C_{102}	−0.076 090	C_{400}	1.592 584	C_{310}	0.248 738
C_{220}	0.451 763	C_{202}	−0.063 746	C_{112}	0.269 327	C_{004}	−0.007 386
				Pt−Xe_2			
C_{200}	0.963 671	C_{110}	0.248 688	C_{002}	0.029 098	C_{300}	−2.804 516
C_{210}	−0.469 580	C_{102}	−0.058 118	C_{400}	2.530 193	C_{310}	0.000 375
C_{220}	−0.169 400	C_{202}	−0.085 159	C_{112}	0.194 849	C_{004}	−0.005 582

TABLE IV. The harmonic frequencies ω_i and vibrational energy levels (v_1, v_2^l, v_3), corresponding to the fundamental frequencies ν_i, overtones, and combination bands, evaluated for the singlet ground state of $Pd-Ng_2$ and $Pt-Ng_2$. Units are given in cm^{-1}.

	$Pd-Ar_2$	$Pd-Kr_2$	$Pd-Xe_2$	$Pt-Ar_2$	$Pt-Kr_2$	$Pt-Xe_2$
ω_1 (σ_g)	98.8	98.7	99.2	202.2	155.8	139.4
ω_2 (π_u)	51.0	46.3	37.9	93.6	64.6	51.8
ω_3 (σ_u)	154.0	165.0	173.1	233.2	197.1	183.0
ν_1 (σ_g)	85.7	92.6	97.7	191.3	150.6	136.0
ν_2 (π_u)	37.1	37.9	36.9	77.7	59.1	48.4
ν_3 (σ_u)	141.3	157.3	166.6	222.2	190.5	182.8
$(2,0^0,0)$	167.2	183.9	194.8	379.9	300.3	271.5
$(0,2^0,0)$	73.3	75.3	73.3	154.8	117.9	96.5
$(0,2^2,0)$	73.8	75.6	73.6	155.1	118.1	96.7
$(0,0^0,2)$	275.6	311.5	331.5	441.7	379.6	364.7
$(1,1^1,0)$	121.8	130.2	134.7	268.3	209.5	184.4
$(0,1^1,1)$	176.4	194.3	202.9	298.8	249.1	230.9
$(1,0^0,1)$	220.0	247.1	262.6	408.7	339.0	317.6

Table IV shows the harmonic frequencies ω_i and low-lying vibrational-rotational energy levels including fundamental frequencies ν_i, overtones, and combination bands for $Pd-Ng_2$ and $Pt-Ng_2$ determined by variational calculations. The harmonic frequencies ω_1, ω_2, and ω_3 correspond to the symmetric stretching, bending, and antisymmetric stretching modes, respectively. The comparison of stretching frequencies of $Pd-Ng_2$ (ω_1 and ω_3) with ω_e of Pd–Ng (in Table I) suggests that Pd–Ar and Pd–Kr bonds in $Pd-Ng_2$ become extensively stronger than the corresponding bonds in Pd–Ng, while the Pd–Xe bond in $Pd-Xe_2$ seems not so changed from the corresponding bond in Pd–Xe diatomic molecule. Interestingly all $Pd-Ng_2$ have a similar harmonic frequency for the symmetric stretching mode, i.e., $\omega_1=98.8\ cm^{-1}$ (Ar), $98.7\ cm^{-1}$ (Kr), and $99.2\ cm^{-1}$ (Xe), but the fundamental frequencies are so different that $\nu_1=85.7\ cm^{-1}$ (Ar), $92.6\ cm^{-1}$ (Kr), and $97.7\ cm^{-1}$ (Xe). On the other hand, the harmonic frequencies for bending mode are different with each other [$\omega_2=51.0\ cm^{-1}$ (Ar), $46.3\ cm^{-1}$ (Kr), and $37.9\ cm^{-1}$ (Xe)], but the fundamental frequencies show similar values, i.e., $\nu_2=37.1\ cm^{-1}$ (Ar), $37.9\ cm^{-1}$ (Kr), and $36.9\ cm^{-1}$ (Xe). The vibrational energy levels for bending modes are described by two quantum numbers, v_2 and l, the latter of which is a vibrational angular quantum number. The overtones for bending mode show a small splitting as to $l=0$ and 2.

Figure 4 shows CCSD(T) counterpoise-corrected potential energy curves for $Pd-Ng_3$ calculated within the D_{3h} point group restriction. The Pd–Ng bond lengths are calculated as 2.901, 2.768, and 2.765 Å, which are much longer than the corresponding ones in $Pd-Ng_2$. The dissociation energies to Pd+3Ng are calculated as 2.78, 8.57, and 20.53 kcal/mol for $Pd-Ar_3$, $Pd-Kr_3$, and $Pd-Xe_3$, respectively, and thus the energy level of $PdNg_3$ is even higher than the energy level of $PdNg_2+Ng$. In order to examine the stability of D_{3h} minimum structure on the potential energy surface, we calculated changes of potential energy along the linearly interpolated C_{2v} path connecting $Pd-Ng_3$ minimum (D_{3h}) and a supermolecule of $Ng'+Pd-Ng_2$ $(D_{\infty h})$, where a leaving Ng′ is separated by 7 Å from Pd. The linear interpolation was performed in terms of Pd–Ng and Pd–Ng′ bond lengths (r_1, r_2) and Ng–Pd–Ng valence angle (θ). At each grid point, the counterpoise corrected interaction energy

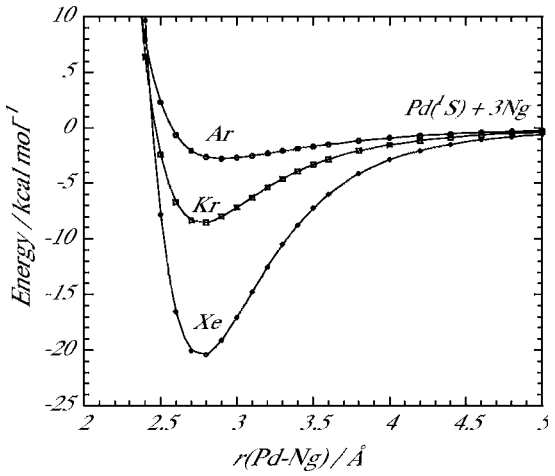

FIG. 4. Potential energy curves for the singlet ground state ($^1A_1'$) of $Pd-Ng_3$ (Ng=Ar,Kr,Xe) in D_{3h} point group as a function of Pd–Ng distance r(PdNg).

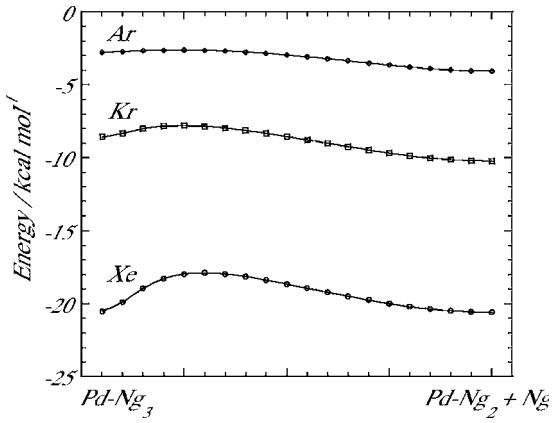

FIG. 5. Change of potential energy along the linearly interpolated path between $Pd-Ng_3$ and $Pd-Ng_2+Ng$ (Ng=Ar,Kr,Xe).

TABLE V. The equilibrium bond length, binding energies, and Mulliken atomic-orbital populations for Pd–5*s* and Pd–4*d* for Pd–Ng_3.

Parameter	Pd–Ar_3	Pd–Kr_3	Pd–Xe_3
r_e (Å)	2.901	2.768	2.765
BE_e (kcal/mol)	2.78	8.57	20.53
n(Pd–5*s*)	0.048	0.104	0.179
n(Pd–4*d*)	9.846	9.764	9.631

was calculated as

$$V_{\mathrm{int,Ng'-Pd-Ng_2}}(r_1,r_2,\theta) = V_{\mathrm{Ng'-Pd-Ng_2}}(r_1,r_2,\theta) - V_{\mathrm{Pd}}(r_1,r_2,\theta) - V_{\mathrm{Ng'}}(r_1,r_2,\theta) - V_{\mathrm{Ng}}(r_1,r_2,\theta)\times 2. \quad (7)$$

Figure 5 shows energy profiles along the linearly interpolated path for Pd–$Ng_3 \rightarrow$ Ng+Pd–Ng_2. In the case of Pd–Kr_3 and Pd–Xe_3, there is an activation barrier to the dissociation of Ng′ atom, although the activation energy is not so large especially for Pd–Kr_3. In the case of Pd–Ar_3, the change of potential energy shows an almost flat feature, indicating that Pd–Ar_2 is coordinatively saturated, and no additional Ar atoms can attach to Pd–Ar_2. Table V summarizes the bond lengths, binding energies, and Mulliken atomic-orbital populations (Pd-5*s* and Pd-4*d*) of the D_{3h} minimum for Pd–Ng_3. As shown in atomic-orbital populations, the hybridizations in 5*s* and 4*d* atomic orbitals are extensively reduced from those in Pd–Ng_2, which may result in less stabilization for the binding of Ng and Pd–Ng_2.

The comparison of Pd–Ng bond lengths and binding energies in Pd–Ng, Pd–Ng_2, and Pd–Ng_3 indicates that the order of Pd–Ng bond strength is Pd–Ng_2 > Pd–Ng > Pd–Ng_3. In particular, the Pd–Ar bond length decreases from 2.797 Å in Pd–Ar to 2.544 Å in Pd–Ar_2 system, and again it increases to 2.901 Å in Pd–Ar_3. This behavior is related to the binding mechanism due to s-d_σ hybridization, which occurs most effectively in a linear geometry. Following the analyses of bond lengths for Ng–MX system by Gerry and co-workers,[21,22] we compare the M–Ng bond lengths in M–Ng, M–Ng_2, and M–Ng_3 species with respect to "van der Waals limit" and "covalent limit." In the present cases of Pd–Ng_n and $PtNg_n$, the bond lengths in van der Waals limit (r_{vdW}) could be expressed as a sum of van der Waals radii of each atom, while those in covalent limit (r_{cov}) correspond to a sum of covalent radii of each atom. Table VI shows comparison of M–Ng bond lengths with values estimated from standard parameters of van der Waals radius[48,49] and covalent radius[50–52] of the respective atoms. As is clearly shown here, bond lengths in van der Waals limit are much larger than the calculated bond lengths, and M–Ng bonds in Pd–Ng_n and Pt–Ng_n can be classified to covalent bonds. Especially, M–Ng bond lengths in Pd–Xe_2, Pt–Ar, Pt–Ar_2, Pt–Kr, and Pt–Kr_2 are very close to the value of covalent limit, and Pt–Xe bond lengths in Pt–Xe and Pt–Xe_2 are even smaller by 0.1–0.2 Å than the covalent limit value. It is noted that there are several variations of covalent radius for Pd and Pt atoms.

In the present study, we have found that the second Ng atom can attach to Pd with much larger binding energy than the first Ng atom. Based on this discovery we decided to perform *ab initio* calculations for the hybrid noble-gas compounds, Xe–Pd–Ng and Xe–Pt–Ng (Ng=He,Ne,Ar,Kr), since the lighter noble-gas atoms are expected to bind with PdXe or PtXe more easily than with Pd or Pt atom. The CCSD(T) counterpoise-corrected potential energies were calculated at 196 points around the minimum energy structure estimated from DFT calculations, and those energies were fitted to the potential energy functions defined in Eq. (4). Then, the equilibrium structures were determined from these fitted surfaces for the respective compounds. At this

TABLE VI. Comparison of M–Ng bond lengths (Å) with values estimated from standard parameters.

	Standard parameters				
Atom	van der Waals radius		Covalent radius		
Ar	1.88[a]		0.98[b]		
Kr	2.00[a]		1.09–1.11[c]		
Xe	2.18[a]		1.30–1.31[c]		
Pd	1.63[d]		1.353[e]		
Pt	1.75[d]		1.365[e]		
	Bond lengths for M–Ng				
	r_{vdW}	r_{cov}	M–Ng	M–Ng_2	M–Ng_3
Pd–Ar	3.51	2.33	2.797	2.544	2.901
Pd–Kr	3.63	2.45	2.643	2.554	2.768
Pd–Xe	3.81	2.66	2.629	2.619	2.765
Pt–Ar	3.63	2.35	2.383	2.352	···
Pt–Kr	3.75	2.47	2.430	2.435	···
Pt–Xe	3.93	2.68	2.500	2.546	···

[a]Reference 48.
[b]Reference 50.
[c]Reference 51.
[d]Reference 49.
[e]Reference 52.

TABLE VII. Expansion coefficients for potential energy surfaces of Xe–Pd–Ng and Xe–Pt–Ng.

				Xe–Pd–He			
C_{200}	0.571 847	C_{110}	−0.029 262	C_{020}	0.061 640	C_{002}	0.009 076
C_{300}	−1.841 254	C_{210}	−0.111 675	C_{120}	−0.081 915	C_{030}	−0.244 791
C_{102}	−0.027 570	C_{012}	−0.031 500	C_{400}	1.581 567	C_{310}	0.062 655
C_{220}	0.169 822	C_{130}	0.124 989	C_{040}	0.345 751	C_{202}	−0.003 817
C_{112}	0.113 516	C_{022}	0.019 911	C_{004}	−0.002 416		
				Xe–Pd–Ar			
C_{200}	0.580 737	C_{110}	−0.018 660	C_{020}	0.207 053	C_{002}	0.009 897
C_{300}	−1.862 862	C_{210}	−0.176 344	C_{120}	−0.195 363	C_{030}	−0.775 559
C_{102}	−0.030 475	C_{012}	−0.042 145	C_{400}	1.712 100	C_{310}	0.083 150
C_{220}	0.326 338	C_{130}	0.286 479	C_{040}	0.996 745	C_{202}	−0.007 208
C_{112}	0.141 890	C_{022}	0.035 060	C_{004}	−0.002 174		
				Xe–Pd–Kr			
C_{200}	0.582 517	C_{110}	0.014 131	C_{020}	0.343 106	C_{002}	0.011 354
C_{300}	−1.837 702	C_{210}	−0.241 928	C_{120}	−0.270 439	C_{030}	−1.166 452
C_{102}	−0.035 112	C_{012}	−0.042 693	C_{400}	1.578 552	C_{310}	0.112 918
C_{220}	0.423 040	C_{130}	0.230 364	C_{040}	1.218 728	C_{202}	−0.007 682
C_{112}	0.149 016	C_{022}	0.015 442	C_{004}	−0.002 311		
				Xe–Pt–He			
C_{200}	1.055 152	C_{110}	0.102 872	C_{020}	0.260 870	C_{002}	0.032 469
C_{300}	−3.031 519	C_{210}	−0.409 645	C_{120}	−0.305 150	C_{030}	−0.914 788
C_{102}	−0.067 882	C_{012}	−0.081 077	C_{400}	2.547 503	C_{310}	0.060 560
C_{220}	1.014 163	C_{130}	0.108 915	C_{040}	1.079 231	C_{202}	−0.068 638
C_{112}	0.216 125	C_{022}	0.023 585	C_{004}	−0.006 913		
				Xe–Pt–Ne			
C_{200}	1.098 791	C_{110}	−0.031 548	C_{020}	0.063 774	C_{002}	0.013 161
C_{300}	−3.052 013	C_{210}	−0.152 506	C_{120}	−0.056 759	C_{030}	−0.302 120
C_{102}	−0.017 805	C_{012}	−0.059 382	C_{400}	1.129 972	C_{310}	0.955 233
C_{220}	0.200 507	C_{130}	−0.148 519	C_{040}	0.610 475	C_{202}	−0.050 905
C_{112}	0.136 762	C_{022}	0.093 259	C_{004}	−0.005 221		
				Xe–Pt–Ar			
C_{200}	1.062 896	C_{110}	0.136 029	C_{020}	0.482 033	C_{002}	0.030 080
C_{300}	−2.981 661	C_{210}	−0.368 670	C_{120}	−0.483 041	C_{030}	−1.515 725
C_{102}	−0.057 426	C_{012}	−0.083 549	C_{400}	1.998 802	C_{310}	0.011 651
C_{220}	0.734 395	C_{130}	0.269 775	C_{040}	1.415 236	C_{202}	−0.080 762
C_{112}	0.257 040	C_{022}	−0.037 139	C_{004}	−0.006 656		
				Xe–Pt–Kr			
C_{200}	1.024 711	C_{110}	0.201 514	C_{020}	0.670 801	C_{002}	0.030 366
C_{300}	−2.888 584	C_{210}	−0.376 946	C_{120}	−0.472 438	C_{030}	−1.975 945
C_{102}	−0.057 970	C_{012}	−0.074 397	C_{400}	2.021 894	C_{310}	−0.452 484
C_{220}	0.448 973	C_{130}	−0.145 197	C_{040}	1.421 083	C_{202}	−0.087 452
C_{112}	0.224 715	C_{022}	−0.061 120	C_{004}	−0.006 522		

stage, we noted that there was no bound state for Xe–Pd–Ne. Table VII shows expansion coefficients for the respective potential energy surfaces for Xe−M−Ng (M=Pd,Pt; Ng =He,Ne,Ar,Kr). Based on these potential energy surfaces, variational calculations were performed to determine vibrational-rotational energy levels using the RVIB3 code. Table VIII summarizes calculated equilibrium bond lengths, binding energies, rotational constants, and fundamental frequencies for these compounds. The respective bond lengths, r_e(Xe−M), r_e(M−Ar), and r_e(M−Kr), are all similar to the corresponding bond lengths in Ng−M−Ng given in Table II, while Pd–He, Pt–He, and Pt–Ne bond lengths are estimated as 2.065, 1.818, and 2.578 Å, respectively. The binding energy for XeM and Ng can be estimated by subtracting the binding energy for Pd–Xe (8.52 kcal/mol) and Pt–Xe (22.10 kcal/mol) given in Table I from the binding energy for Xe+M+Ng→Xe−M−Ng given in Table VIII. The thus estimated binding energies are 1.12 kcal/mol (XePd–He), 4.02 kcal/mol (XePd–Ar), 6.94 kcal/mol (XePd–Kr), 5.46 kcal/mol (XePt–He), 0.50 kcal/mol (XePt–Ne), 9.75 kcal/mol (XePt–Ar), and 14.20 kcal/mol (XePt–Kr). Taking into account zero–point vibrational energy in the respective compounds, the corresponding binding energies are reduced to 0.55, 3.71, 6.64, 4.17, 0.23, 9.31, and 13.83 kcal/mol, respectively. Although the binding strength in XePd–He and XePt–Ne seems fairly weak, the other

TABLE VIII. The equilibrium bond lengths, binding energies, rotational constants, and fundamental frequencies ν_i, evaluated for the singlet ground state of Xe–M–Ng (M=Pd, Pt; Ng=He, Ne, Ar, Kr).

	Xe–Pd–Ng			Xe–Pt–Ng			
Parameter	He	Ar	Kr	He	Ne	Ar	Kr
r_e(Xe–M) (Å)	2.599	2.598	2.603	2.509	2.495	2.513	2.525
r_e(M–Ng) (Å)	2.065	2.553	2.574	1.818	2.578	2.405	2.468
BE_e (kcal/mol)	9.64	12.54	15.46	27.56	22.60	31.85	36.30
BE_0 (kcal/mol)	8.89	12.05	14.98	26.02	22.08	31.16	35.68
B_e (GHz)	1.1350	0.5364	0.3647	0.9594	0.6905	0.5536	0.3849
B_0 (GHz)	1.1190	0.5329	0.3597	0.9562	0.6824	0.5519	0.3840
ν_1 (cm^{-1})	161.4	160.0	164.1	174.5	181.6	162.6	183.3
ν_2 (cm^{-1})	78.7	38.4	37.2	186.5	44.6	62.3	53.4
ν_3 (cm^{-1})	124.0	99.6	95.1	450.6	70.3	195.3	143.5

hybrid compounds, Xe–Pd–Ar, Xe–Pd–Kr, Xe–Pt–He, Xe–Pt–Ar, Xe–Pt–Kr, have a sufficiently large binding energy, and they are good candidates as new noble-gas compounds to be detected in the experiment.

Finally we provide brief considerations on the possibility of the existence of nickel–noble-gas compounds. A nickel atom belongs to the same group of Pd and Pt in the Periodic Table, although their electronic ground states are different from each other, i.e., ^3F with d^8s^2 (Ni), ^1S with d^{10} (Pd), and ^3D with d^9s^1 (Pt). Through calculations for Pd–Ng_n and Pt–Ng_n compounds, it is verified that only ^1S state with d^{10} configuration is stabilized by the binding with Ng atoms. This result can be related to the stabilization mechanism due to the s-d_σ hybridization. Burda *et al.* already pointed out that the diatomic Ni–Xe compound is not bound,[27] but it is not yet clear about the stability of Ni–Ng_2 because the second M–Ng binding has been found to be stronger for both Pd and Pt compounds; the binding energies were evaluated as 8.52 and 21.49 kcal/mol for Pd–Xe and Xe–Pd–Xe, respectively, and 22.10 and 44.92 kcal/mol for Pt–Xe and Xe–Pt–Xe, respectively. In the case of Pt–Ng_n, the binding energy should be reduced by considering the excitation energy for ^1S of Pt atom relative to the ^3D ground state in the dissociation limit, Pt+nNg. Similarly, the binding energy for Ni–Ng_n should be estimated relative to the dissociation limit, Ni (^3F)+nNg. The experimental excitation energy for ^1S state of Ni atom relative to the ground $^3F_4$ state is reported as 42.1 kcal/mol,[53] which is much larger than the expected stabilization energy for Ni–Ng_2. This consideration suggests that it is difficult to detect Ni–Ng_2 compounds in the experiment.

IV. CONCLUDING REMARKS

We have examined the possibility of new noble-gas compounds with Pd and Pt atoms by applying the CCSD(T) method with the Douglas-Kroll relativistic scheme. We used all-electron relativistic basis sets, augmented with the correlated sets, to take into account both relativistic effects and electron correlation effects quantitatively. The calculations give the expected trend of higher binding energies for the heavier noble-gas xenon. It is also shown that Pt–Ng binding is much stronger than the corresponding Pd–Ng bonding both in terms of bond length and binding energy. The Pt–Ng bond lengths are smaller than the corresponding Pd–Ng bond lengths, which is linked with the stronger relativistic effect in Pt and is a consequence of relativistic bond length contraction.

It is found that Pd–Ar_2, Pd–Kr_2, and Pd–Xe_2 have sufficiently large binding energies of 4.01, 10.17, and 21.49 kcal/mol, respectively. These species take linear geometry as the minimum in which the second Ng atom attaches to Pd atom with a larger binding energy than the first Ng atom. The binding mechanism in these compounds can be explained by the s-d_σ hybridization in Pd atom. The binding energies for the lighter noble-gas atoms and PdXe or PtXe are also examined by the same computational methods, and we show that the hybrid compounds, Xe–Pd–Ar, Xe–Pd–Kr, Xe–Pt–He, Xe–Pt–Ar, and Xe–Pt–Kr, also have a sufficient binding energy. The rotational constants and fundamental frequencies for these species are also determined by variational calculations. We hope that our calculations will motivate the experimentalists to synthesize these new noble-gas compounds.

ACKNOWLEDGMENTS

One of the authors (T.T) would like to thank Dr. Stuart Carter for providing a copy of the RVIB3 program. Another author (Y.T.) gives thanks to Japan Society for the Promotion of Science for Research Fellowships for Young Scientist and would also like to express her gratitude to Professor Y. Okamoto (Nagoya University) for continuous encouragements. The present work was supported in part by an allocation of computing resources from the Institute of Statistical Mathematics in Tokyo and the grant from the Ministry of Education, Science and Culture, and Sports of Japan.

[1] N. Bartlett, Proc. Chem. Soc., London **1962**, 218.
[2] W. Koch, J. R. Collins, and G. Frenking, Chem. Phys. Lett. **132**, 330 (1986).
[3] G. Frenking, W. Koch, J. Gauss, and D. Cremer, J. Am. Chem. Soc. **110**, 8007 (1988).
[4] G. Frenking and D. Cremer, *Structure and Bonding* (Springer, Heidelberg, 1990), Vol. 73, p. 17.
[5] C. A. Thompson and L. Andrews, J. Am. Chem. Soc. **116**, 423 (1994).
[6] A. Veldkamp and G. Frenking, Chem. Phys. Lett. **226**, 11 (1994).
[7] Y. Ono and T. Taketsugu, Chem. Phys. Lett. **385**, 85 (2004).

[8] Y. Ono and T. Taketsugu, J. Chem. Phys. **120**, 6035 (2004).
[9] Y. Ono and T. Taketsugu, J. Phys. Chem. A **108**, 5464 (2004).
[10] Y. Ono and T. Taketsugu, Monatsch. Chem. **136**, 1087 (2005).
[11] P. Pyykkö, J. Am. Chem. Soc. **117**, 2067 (1995).
[12] D. Schröder, H. Schwarz, J. Hrušák, and P. Pyykkö, Inorg. Chem. **37**, 624 (1998).
[13] P. Pyykkö and J.-P. Desclaux, Acc. Chem. Res. **12**, 276 (1979).
[14] P. Pyykkö, Chem. Rev. (Washington, D.C.) **88**, 563 (1988).
[15] S. Seidel and K. Seppelt, Science **290**, 117 (2000).
[16] W.-P. Hu and C.-H. Huang, J. Am. Chem. Soc. **123**, 2340 (2001).
[17] C. J. Evans and M. C. L. Gerry, J. Chem. Phys. **112**, 1321 (2000).
[18] C. J. Evans and M. C. L. Gerry, J. Chem. Phys. **112**, 9363 (2000).
[19] C. J. Evans, A. Lesarri, and M. C. L. Gerry, J. Am. Chem. Soc. **122**, 6100 (2000).
[20] C. J. Evans, D. S. Rubinoff, and M. C. L. Gerry, Phys. Chem. Chem. Phys. **2**, 3943 (2000).
[21] J. M. Michaud, S. A. Cooke, and M. C. L. Gerry, Inorg. Chem. **43**, 3871 (2004).
[22] J. M. Thomas, N. R. Walker, S. A. Cooke, and M. C. L. Gerry, J. Am. Chem. Soc. **126**, 1235 (2004).
[23] S. A. Cooke and M. C. L. Gerry, J. Am. Chem. Soc. **126**, 17000 (2004).
[24] C. C. Lovallo and M. Klobukowski, Chem. Phys. Lett. **368**, 589 (2003).
[25] T. K. Ghanty, J. Chem. Phys. **123**, 074323 (2005).
[26] T. K. Ghanty, J. Chem. Phys. **124**, 124304 (2006).
[27] J. V. Burda, N. Runeberg, and P. Pyykkö, Chem. Phys. Lett. **288**, 635 (1998).
[28] Y. Ono, T. Taketsugu, and T. Noro, J. Chem. Phys. **123**, 204321 (2005).
[29] S. Carter and N. C. Handy, Mol. Phys. **57**, 175 (1986).
[30] S. Carter and N. C. Handy, Comput. Phys. Rep. **5**, 117 (1986).
[31] H.-J. Werner, P. J. Knowles, R. D. Ramos *et al.*, MOLPRO, Version 2002.6, a package of *ab initio* programs designed, University College Cardiff Consultants Limited, Wales, UK, 2002.
[32] N. Douglas and N. M. Kroll, Ann. Phys. (N.Y.) **82**, 89 (1974).
[33] B. A. Hess, Phys. Rev. A **33**, 3742 (1986).
[34] T. Tsuchiya, M. Abe, T. Nakajima, and K. Hirao, J. Chem. Phys. **115**, 4463 (2001).
[35] Y. Osanai, M. Sekiya, T. Noro, and T. Koga, Mol. Phys. **101**, 65 (2003).
[36] T. Noro, M. Sekiya, and T. Koga, Theor. Chem. Acc. **98**, 25 (1997).
[37] M. Sekiya, T. Noro, T. Koga, and H. Matsuyama, J. Mol. Struct.: THEOCHEM **451**, 51 (1998).
[38] M. Sekiya, T. Noro, Y. Osanai, and T. Koga, Theor. Chem. Acc. **106**, 297 (2001).
[39] http://setani.sci.hokudai.ac.jp/sapporo/
[40] S. F. Boys and F. Bernardi, Mol. Phys. **19**, 553 (1970).
[41] G. Simons, R. G. Parr, and J. M. Finlan, J. Chem. Phys. **59**, 3229 (1973).
[42] J. Sansonetti, W. Martin, and S. Young, *Handbook of Basic Atomic Spectroscopic Data*, Version 1.00 (National Institute of Standards and Technology, Gaithersburg, MD, 2003) http://physics.nist.gov/Handbook
[43] J. Raab and B. O. Roos, in *Advances in Quantum Chemistry*, edited by J. R. Sabin, E. Brandas, and L. B. Oddershede (Academic, New York, 2005), Vol. 48, p. 421.
[44] P. E. M. Siegbahn, M. R. A. Blomberg, and M. Svensson, J. Phys. Chem. **97**, 2564 (1993).
[45] M. R. A. Blomberg, P. E. M. Siegbahn, and M. Svensson, Inorg. Chem. **32**, 4218 (1993).
[46] C. W. Bauschlicher, Jr., S. R. Langhoff, and H. Partridge, J. Chem. Phys. **94**, 2068 (1991).
[47] A. J. Lupinetti, V. Jonas, W. Thiel, S. H. Strauss, and G. Frenking, Chem.-Eur. J. **5**, 2573 (1999).
[48] P. Pyykkö, Chem. Rev. (Washington, D.C.) **97**, 597 (1997).
[49] A. Bondi, J. Phys. Chem. **68**, 441 (1964).
[50] P. Pyykkö, Science **290**, 64 (2000).
[51] N. Bartlett and F. O. Sladky, in *Comprehensive Inorganic Chemistry*, edited by J. C. Bailar, H. J. Emeléus, R. Nyholm, and A. F. Trotman-Dickenson (Pergamon, Oxford, 1973), p. 213.
[52] L. Pauling and B. Kamb, Proc. Natl. Acad. Sci. U.S.A. **83**, 3569 (1986).
[53] U. Litzén, J. W. Brault, and A. P. Thorne, Phys. Scr. **47**, 628 (1993).